JOURNAL OF NATURAL REMEDIES
DOI: 10.18311/jnr/2025/49704

SHORT COMMUNICATION

Exploring Phytochemicals for Inhibitory Potential against Key Rheumatoid Arthritis Receptors and Cytokines: An *In Silico* Approach

Preeti Maan[1,2], Shilpi Chauhan[2], Nisha Gupta[3] and Dimpy Rani[1*]

[1]Department of Pharmacy, School of Healthcare and Allied Sciences, GD Goenka University, Gurugram – 122103, India; dimpy1990@gmail.com

[2]Lloyd Institute of Management and Technology, Greater Noida – 201306, Uttar Pradesh, India

[3]IIMT College of Pharmacy, Greater Noida – 201310, Uttar Pradesh, India

Abstract

Background: Rheumatoid Arthritis **(**RA**)** is an autoimmune disease which not only affects the synovial joints but also leads to other co-morbidities. Existing treatments provide only symptomatic relief to patients. This highlights the need for safer and more effective natural lead compounds. **Aim:** To identify potential natural lead compounds for RA by virtually screening selected phytoconstituents against key inflammatory and immunological targets. **Methods:** In urge to search a natural lead candidate, a virtual screening was performed with a total of 27 phytoconstituents against cyclooxygenase-1 (COX-1), cyclooxygenase-2 (COX-2), interleukin-6 (IL-6), Janus kinase-1 (JAK-1), Janus kinase-2 (JAK-2), mitogen-activated protein kinase-14 (MAPK-14), matrix metalloproteinase-9 (MMP9), and tissue necrosis factor-α (TNF-α) using PyRx software. Their ADME prediction was performed using SwissADME. Further, Molinspiration was used to determine the bioactivity score of the selected phytoconstituents as G-Protein Coupled Receptors (GPCR) ligand, Kinase Inhibitor (KI), Ion Channel Modulator (ICM), Protease Inhibitor (PI), Nuclear Receptor Ligand (NRL), and Enzyme Inhibitor (EI). The toxicity of these phytoconstituents was also predicted with the Protox-II web server. **Results:** The docking results displayed that hesperidin, sanguinarine, hecogenin, berberine, naringenin, genistein, piperine, and epicatechin-3-gallate have better binding affinity than the standard drug methotrexate with all the studied receptors. Most of the molecules showed acceptable druglikeness and leadlikeness properties and followed Lipinski's rule of five. All these molecules were found to have moderate activity as GPCR ligands, KI, ICM, PI, NRL, and EI. Further, the toxicity prediction gave promising results. **Conclusion:** The results revealed that these bioactive compounds can provide novel lead candidates that might modulate immunological factors, which in turn prevent rheumatoid arthritis.

Major Findings: The virtual screening filtered out eight phytoconstituents, hesperidin, sanguinarine, hecogenin, berberine, naringin, genistein, piperine, and epicatechin-3-gallate, which possessed good binding affinity with all the studied receptors. These molecules were predicted to have good oral absorption with immunomodulation properties.

Keywords: ADMET, Molecular Docking, Molinspiration, Protox-II, Phytoconstituents, Rheumatoid Arthritis

Abbreviations: COX-1 = Cyclooxygenase-1; COX-2 = Cyclooxygenase-2; EI= Enzyme inhibitor; GPCR = G-protein coupled receptors; ICM = Ion channel modulator; IL-6 = Interleukin-6; JAK-1= Janus kinase-1; JAK-2 = Janus kinase-2; KI = Kinase inhibitor; MAPK-14 = Mitogen-activated protein kinase-14; MMP-9 = Matrix Metallopeptidase-9; NRL = Nuclear receptor ligand; PI = Protease inhibitor; RA = Rheumatoid arthritis; TNF-α = Tissue necrosis factor-α

1. Introduction

Rheumatoid Arthritis (RA) is a chronic, autoimmune disease that affects synovial joints which resulting in bone and cartilage damage on progression[1]. Though it is a disease of joint destruction but it also affects other organs like lungs[2], digestive system, heart, and nervous system[3], which leads to an increase in mortality rate due

*Author for correspondence

Article Received on: 05.05.2025 Revised on: 26.11.2025 Accepted on: 05.12.2025

to RA. According to the World Health Organisation, 18 million individuals had rheumatoid arthritis in 2019. Approximately 70% of persons with rheumatoid arthritis are women, and 55% are above the age of 55[4]. According to the aetiology and pathogenesis of RA, during the pre-rheumatic arthritis phase, the overproduction and accumulation of pro-inflammatory mediators such as Interleukins (ILs) and Tissue Necrosis Factor (TNF-α) and environmental factors (smoking, air pollution, unbalanced diet and occupational dust, *etc.*) might lead to the formation of modified self-antigens by a process called citrullation[5]. These citrullated proteins are not recognised as self-structures by the immune system. These citrullated proteins are carried to the lymph node by antigen-presenting cells, which results in activation of T cells and B cells. These B cells get to proliferate and generate Anti-Citrullated Protein Autoantibodies (ACPA) and Rheumatoid Factor (RF). The presence of these substances is a mark of this disease[6]. All these immunological processes also occur in the joint synovium and synovial fluids. During this process, synovial macrophages release cytokines and pro-inflammatory mediators, which stimulate the abnormal proliferation of osteoclasts and Fibroblast-Like Synoviocytes (FLS)[7], thus leading to cartilage degradation and bone erosion. FLS not only stimulates the NF-κB signalling pathway but also produces Matrix Metalloproteinase (MMP). Both of them increase osteoclast activity, leading to cartilage degeneration and bone erosion. Currently, multiple signal transduction pathways involved in RA are identified, like the nuclear transcription factor (NF-κB) signalling pathway, Mitogen-Activated Protein Kinase (MAPK) signalling pathway, Janus kinase/signal transduction and transcription activation protein (JAK/STAT) signalling pathway, and phosphoinositide 3-kinase/protein kinase B (PI3K/AKT) signalling pathway[8] (Figure 1). The inhibition of the TNF-α signalling pathway reduces NF-κB overexpression and allied inflammatory mediators, making it a latent target for drug design for inflammatory diseases. Furthermore, inhibitors of the Mitogen-Activated Protein Kinases (MAPKs) have also been of much interest because MAPKs are key regulators of pro-inflammatory cytokine production. Moreover, PI3K/AKT signalling pathway influences FLS cells' abnormal proliferation, synovial inflammation, and osteoclast generation and differentiation[9]. Clinical investigations have revealed that Janus Kinase 1 (JAK1) mediated signalling is important in the synovial response in rheumatoid arthritis. As a result, JAK1 inhibition is recognised as a key therapeutic strategy in the treatment of rheumatoid arthritis. As a result, drugs that specifically block JAKs have gained a lot of attention as probable novel therapies for the treatment of RA in recent years[10].

While there is currently no cure for RA, the various therapy alternatives can help to reduce symptoms and enhance survival. First and foremost, Non-Steroidal Anti-Inflammatory Drugs (NSAIDs) are used to relieve swelling, pain, and inflammation[11]. NSAIDs inhibit cyclooxygenase (COX)-2, which blocks PG production at sites of inflammation, whereas inhibiting COX-1 in other tissues (gastroduodenal mucosa and platelets) results in NSAID-related side effects such as gastrointestinal ulceration and bleeding[12]. Besides that, corticosteroids, like glucocorticoids, are a type of powerful anti-inflammatory drug, but they have side effects including nausea, gastrointestinal distress, abdominal pain, ulcers, skin rash, hypersensitivity reactions, elevated blood glucose and blood pressure, vomiting, and diarrhoea in patients[13]. The long-term use of synthetic drugs has a variety of negative consequences. As a result, the current medical scenario favours traditional herbal plants. Phytoconstituents have a broad range of biological properties, including anti-inflammatory activity, which has gained them a lot of attention. Further, the computational tools have also shortened the pathway to discovering new therapeutic leads[14]. The current *in silico* study aims to evaluate the inhibitory potentials of 27 selected phytoconstituents against eight key RA receptors and cytokines to identify effective modulators. The best-hit compounds were further evaluated for druglikeness, leadlikeness, and ADMET properties.

2. Materials and Methods

2.1 Characterisation of Target Receptor Proteins

ProtParam web server[15] as used to compute the physicochemical properties like the theoretical pI, molecular weight, total number of amino acids, amino acid composition, instability index, atomic composition, aliphatic index, extinction coefficient,

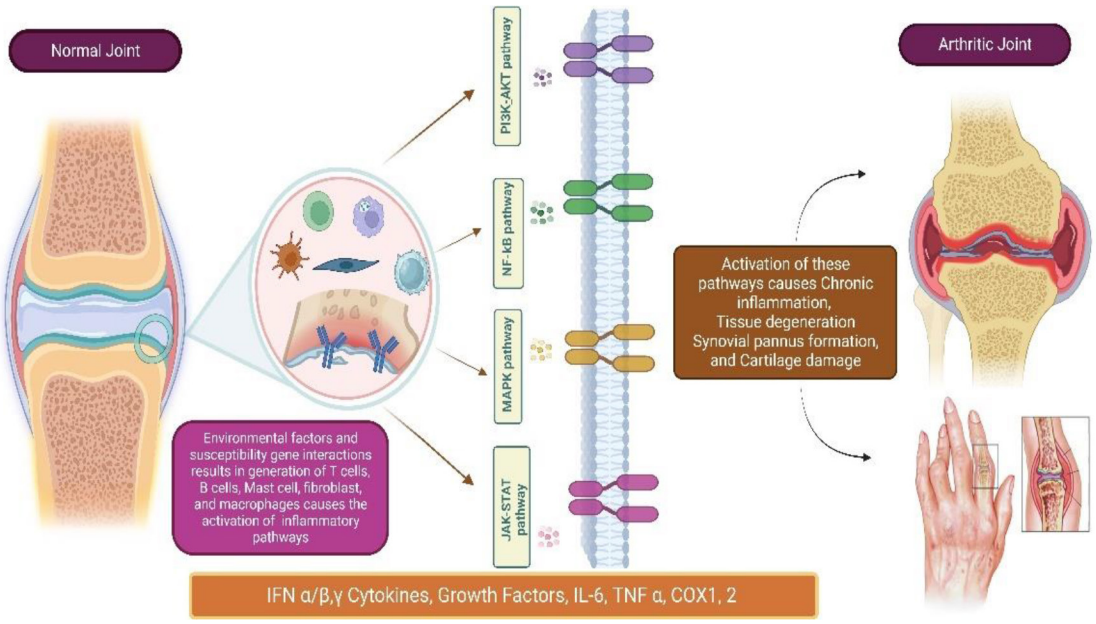


Figure 1. Pathogenesis of rheumatoid arthritis and therapeutic targets.

and grand average of hydropathicity (GRAVY) of all proteins under study. *i.e.*, COX-1, COX2, IL-6, JAK1, JAK2, MAPK-14, MMP9, TNF-α[16-18].

2.2 Structure Retrieval and Preparation of Targets

X-ray diffraction crystal structures of all the receptors COX-1 (pdb: 3n8z)[19], COX-2 (pdb: 4ph9)[20], IL-6 (pdb: 1alu)[21], JAK-1 (pdb: 4ehz)[22], JAK-2 (pdb: 3e62)[23], MAPK-14 (pdb: 4f9y)[24], MMP9 (pdb: 3esm)[25] and TNF-α (pdb: 2az5)[26] were obtained from RCSB Protein Databank[27]. Prior to docking, the native ligands and water molecules were removed. Additionally, the polar hydrogens were added using UCSF Chimera 1.13.1[28]. Dockprep files were prepared, which were further used by AutoDock Vina embedded in PyRx software for virtual screening[29]. The binding affinity of the studied molecules was also compared with the gold standard drug (methotrexate) for rheumatoid arthritis treatment.

2.3 Collection and Preparation of Ligands

The plants used in marketed herbal formulations of rheumatoid arthritis were enlisted for the study. Molecular docking analysis was performed on 27 phytoconstituents, mainly including flavonoids, triterpenoids, and alkaloids present in these plants, based on their anti-rheumatoid arthritis activity. Three-dimensional structures of all these compounds were regained from the PubChem Database[30] (Figure 2). Three-dimensional structures of internal ligands of receptor proteins were also downloaded from PubChem. All the structures were combined in .sdf format by using Open Babel, version 2.3.1[31].

2.4 Virtual Screening using the PyRx0.8

The virtual screening of all the plant constituents was performed by PyRx0.8 software (AutoDock Vina wizard)[32-35]. The proteins were considered as rigid bodies, whereas phytoconstituents were regarded as flexible. The docking process was validated by redocking the respective modulators for assurance of the binding of ligands in the active pocket of the protein. The configuration file for the grid parameters was generated using the Auto Grid engine in PyRx. The grid box was set over the active site of receptors with the dimensions given in Table 1.

The binding modes and the exhaustiveness for docking were set as 10 and 100, respectively. The highest binding energy with the least RMSD having conformation was considered the best conformation. Discovery Studio visualizer was used for the analysis of docking results[36].

2.5 ADMET Analysis

Effective ADMET characteristics at the therapeutic dosage are just as important as effectiveness against the

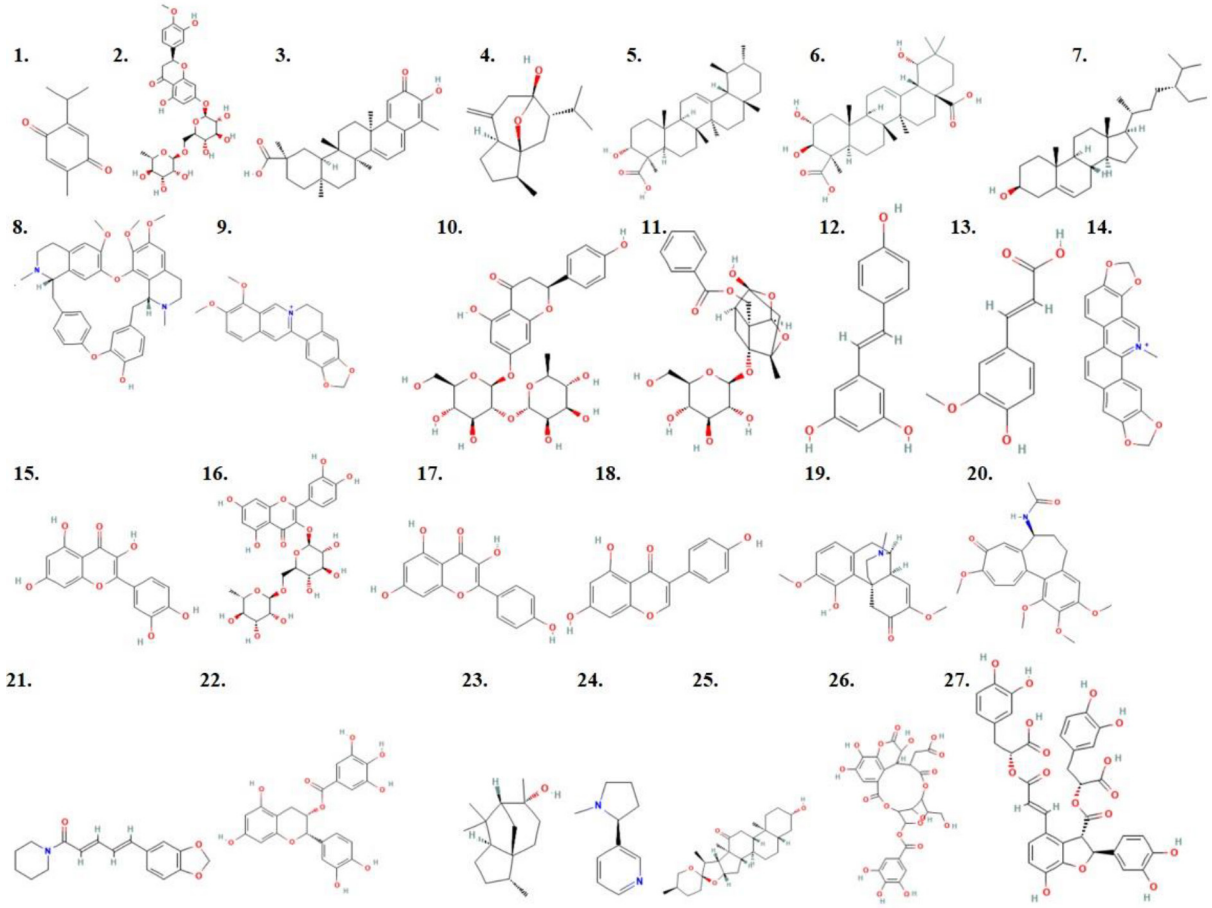


Figure 2. 2D structures of 27 phytoconstituents used in this study: **(1)** Thymoquinone, **(2)** Hesperidin, **(3)** Celastrol, **(4)** Curcumol, **(5)** β-Boswellic acid, **(6)** Bartogenic acid, **(7)** β-Sitosterol, **(8)** Berberine, **(9)** Berbamine, **(10)** Naringin, **(11)** Paeoniflorin, **(12)** Resveratrol, **(13)** Ferulic acid, **(14)** Sanguinarine, **(15)** Quercetin, **(16)** Rutin, **(17)** Kaempferol, **(18)** Genistein, **(19)** Sinomenin, **(20)** Colchicine, **(21)** Piperine, **(22)** Epicatechin-3-gallate, **(23)** Cedrol, **(24)** Nicotine, **(25)** Hecogenin, **(26)** Chebulanin, **(27)** Salvianolic acid B.

Table 1. Dimensions of the grid box

Receptor	Center coordinates			Center size		
	x	y	z	x	y	z
COX-1	-17.34	48.82	7.90	24.32	22.44	24.17
COX-2	12.43	24.41	23.36	27.45	28.98	30.41
IL-6	-5.98	-13.53	4.05	26.07	28.53	16.52
JAK-1	4.59	57.05	2.06	20.04	23.73	19.19
JAK-2	35.74	40.78	35.67	20.81	15.04	20.48
MAPK-14	25.63	13.79	11.75	26.07	23.20	20.93
MMP9	0.18	48.25	23.04	22.31	20.95	24.83
TNF-α	-21.63	70.05	35.46	21.41	19.79	14.76

therapeutic target for a promising drug candidate. So, the SwissADME web server (http://www.swissadme.ch/) was used to screen the selected phytoconstituents for the prediction of simple physicochemical properties[37-39] like molecular weight, number of heavy atoms, and total polar surface area[40]. Other than these

properties, lipophilicity (Average Log $P_{o/w}$ of iLOGP[41], XLOGP3[41], WLOGP[43], MLOGP[44,45], SILICOS-IT[46] models), water solubility (predicted with three models: ESOL[47], Ali[48] and SILICOS-IT[46]) and pharmacokinetics of molecules were also computed with this web server[49]. This web server was also used to identify a potential lead compound with lead-likeness and drug-likeness properties. These properties were predicted with the rules implemented by Egan[50], Ghose[51], Lipinski[52], Muegge[53] and Veber[54,55].

2.6 Bioactivity Score and Bioavailability Radar

The bioactivity score of the selected molecules was determined by using online Molinspiration software[56,57]. The bioactivity was scored as G-Protein Coupled Receptors (GPCR) ligand, Kinase Inhibitor (KI), Ion channel modulator (ICM), Protease Inhibitor (PI), Nuclear Receptor Ligand (NRL), Enzyme Inhibitor (EI). The bioavailability radar of the selected phytoconstituents was determined by using SwissADME, which is used to determine the oral bioavailability of the molecule[58].

2.7 Toxicity Analysis

A web server, ProTox-II, was employed to predict the toxicity of molecules in terms of hepatotoxicity, immunotoxicity, carcinogenicity, mutagenicity, and cytotoxicity[59,60]. Toxicity profiling may help to reduce potential hazards during preclinical development.

3. Result and Discussion

3.1 Target Receptor Protein's Characterisation

The physicochemical properties of all the proteins were predicted from the ProtParam web-based tool[15], and the results were compiled in Table 2. In this table, the theoretical pI (isoelectric point) and molecular weight were calculated from a specified Swiss-Prot/TrEMBL entry or a user-entered AA sequence. These parameters give an idea about the distance travelled by the protein in a 2D gel. The extinction coefficient of protein was calculated from the molar extinction coefficient of tyrosine, cystine, and tryptophan at a certain wavelength. This parameter is an indication of light absorbed by a protein. It helped out during the purification of protein by spectrophotometry. Further, the instability index gave an idea about the stability of the protein in a test tube. According to this server, a protein having an instability index less than 40 is assumed as stable *in vitro*. The relative volume occupied by aliphatic amino acids, *i.e.,* valine, alanine, leucine, and isoleucine side chains, is used for the calculation of the aliphatic index of a protein. It is a positive indication of the thermostability of globular proteins. Moreover, the Grand Average of Hydropathy (GRAVY) is the measurement of the average hydrophilicity of the protein. A protein is assumed to be hydrophilic if the GRAVY value is less than zero. According to the results, all the studied proteins are hydrophilic in nature.

3.2 Virtual Screening and Molecular Docking

Rheumatoid arthritis is an autoimmune and inflammatory disease. So, it is necessary to do screening of molecules against the inflammatory receptors as well as cytokine factors to find a suitable drug candidate for the treatment of this disease. Hence, the selected plant constituents were screened against these receptor proteins and cytokines COX-1, COX-2, IL-6, JAK-1, JAK-2, MAPK-14, MM9P, and TNF-α using Autodock 4.2[29] assembled in Pyrx0.8[32]. Before docking, the process was validated by redocking of the co-crystallised ligand to verify the docking of molecules inside the active pocket sites of the target proteins with possible interactions. All the docked ligands showed less deviation from the actual co-crystallised complex except the ligand of TNF-α, due to its highly flexible structure, although it was bound in the same cavity (Figure 3). The results of molecular docking were compiled as the binding affinity in terms of kcal/mol in Table 3. A modulator with a lower value (high in negative) of free binding energy and low RMSD was supposed as the best conformation. Out of 27 molecules, eight phytoconstituents have a binding affinity of more than -6 kcal/mol against all the studied receptors. Further, hesperidin was found to be the most promising compound because it showed the highest binding affinity with most of the receptors, although with other targets, its binding affinity was comparable to the best-ranked compounds also. Interestingly, hesperidin has a binding affinity higher than the standard drug, methotrexate, with all the receptors. Despite hesperidin, hecogenin was found to be the best

Table 2. Physicochemical properties of all the receptor proteins used in this study

S. No.	Properties	COX-1	COX-2	IL-6	JAK-1	JAK-2	MAPK-14	MMP9	TNF-α
1	Molecular weight	68861.34	69013.13	23718.22	133277.04	130673.55	41293.29	78458.23	25644.42
2	Total no. of amino acids	600	604	212	1154	1132	360	707	233
3	Total atoms	9646	9668	3348	18687	18288	5805	10836	3633
4	Chemical formula	$C_{3145}H_{4786}N_{824}O_{862}S_{29}$	$C_{3128}H_{4802}N_{822}O_{889}S_{27}$	$C_{1049}H_{1685}N_{283}O_{321}S_{10}$	$C_{5930}H_{9332}N_{1612}O_{1747}S_{66}$	$C_{5848}H_{9096}N_{1582}O_{1705}S_{57}$	$C_{1854}H_{2898}N_{494}O_{544}S_{15}$	$C_{3517}H_{5298}N_{958}O_{1035}S_{28}$	$C_{1152}H_{1825}N_{313}O_{337}S_{6}$
5	Theoretical pI	7.00	7.00	6.17	7.48	6.82	5.48	5.69	6.44
6	Extinction coefficient	90480 at Abs 0.1% 1.314#	73980 Abs 0.1% 1.072#	10220 Abs 0.1% (=1 g/l) 0.431#	151550 Abs 0.1% (=1 g/l) 1.137#	151635 Abs 0.1% (=1 g/l) 1.160#	50100 Abs 0.1% (=1 g/l) 1.213#	118355 Abs 0.1% (=1 g/l) 1.509#	21680 Abs 0.1% (=1 g/l) 0.845#
7	Instability index	48.33	39.55	57.70	49.76	47.71	43.64	41.10	40.75
8	Aliphatic index	82.37	81.34	87.50	80.82	82.68	95.08	65.13	98.37
9	Charge	Negative	Negative	Negative	Positive	Negative	Negative	Negative	Negative
10	Grand average of hydropathicity (GRAVY)	-0.235	-0.303	-0.271	-0.521	-0.433	-0.261	-0.394	-0.047

#Assumes all pairs of Cys residues form cystines

molecule against COX-1 and TNF-α. Sanguinarine and genistein showed the highest binding affinity against JAK-2 and MAPK-14. The binding affinities of these molecules surpassed the binding affinities of the internal ligand of respective targets also.

Further, the binding poses of the best conformation of the most active phytoconstituent with the receptors were analysed with Discovery Studio Visualizer. The results indicated the presence of promising inhibitors inside the pockets of the respective target with various types of interactions like hydrogen bonds, hydrophobic interactions, and electrostatic interactions. The ligand-protein interactions of the best-ranked compound with all the studied targets are presented in Figure 4-11. The binding poses showed that hecogenin interacts with the COX-1 (pdb:3n8z) receptor with alkyl-type hydrophobic interactions with LEU93, LEU112, VAL116, VAL119, ARG120, LEU123, LEU357 residues; π-alkyl interaction with TRP100 amino acid and van der Waals interactions with amino acids ARG83, LEU115, PHE470, GLY471 (Figure 4).

The interactions of hesperidin in the active site of COX-2 (pdb: 4ph9) were stabilized by hydrogen bonding with residues TYR386, SER120, ARG121, TYR356; one amide-π stacked interactions with GLY527 and ALA528; alkyl and π-alkyl hydrophobic interactions with LEU385, MET523, and VAL117, TRP388, VAL524, ALA528, LEU532; and van der Waals interactions with VAL350 and SER531 amino acids (Figure 5).

Further, hesperidin was found to be the most active compound with IL-6 (pdb: 1alu). This compound interacted with the target receptor by hydrogen bonding with GLN75, SER176; carbon-hydrogen bonding with ARG179; an electrostatic π-cation bonding with ARG179; alkyl hydrophobic interactions with LEU178, ARG182; and π-alkyl interactions with LEU178 and ARG179 (Figure 6).

Moreover, this compound was the most promising compound against JAK-1 (pdb: 4ehz) also. With this target protein, the interactions of hesperidin were supported by hydrogen bonds with residues GLY884, HIS885, PHE886, GLY887, LEU959, ASN1008; carbon-hydrogen bond with PHE958; π-sulfur with MET956; π-σ bond with LEU881; alkyl hydrophobic interactions with LEU1024; and π-alkyl hydrophobic interactions with VAL889, ALA906, LEU1010 (Figure 7).

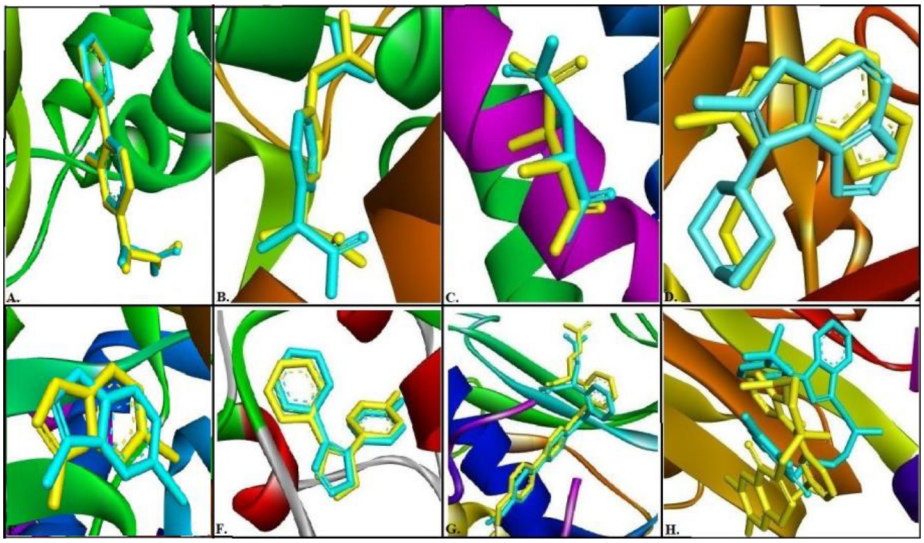


Figure 3. Docked poses and superimposed co-crystal of internal ligands of all the receptor proteins: **(A)** 3n8z, **(B)** 4ph9, **(C)** 1alu, **(D)** 4ehz, **(E)** 3e62, **(F)** 4f9y, **(G)** 3esm, **(H)** 2az5. Cyan colour embodies the docked ligand, and yellow colour embodies the co-crystallised ligands.

Table 3. The binding affinity (in kcal/mol) of 27 phytoconstituents with all proteins under study

S. No.	Compounds	Binding affinity in kcal/mol							
		COX-1	COX-2	IL-6	JAK-1	JAK-2	MAPK-14	MMP9	TNF-α
1	Hesperidin	-8	-9	-7.3	-11.4	-9.1	-8.1	-11	-6.9
2	Sanguinarine	-8.4	-7.8	-7.1	-10.2	-10.1	-8.2	-8	-8
3	Hecogenin	-8.8	-8	-6.9	-9.5	-9.1	-6.3	-8.9	-8.3
4	Berberine	-7.4	-7.4	-6.7	-9.4	-8.6	-8.6	-7.4	-7.1
5	Naringin	-7.5	-8.8	-6.7	-10.8	-8.6	-8.4	-9.7	-6.4
6	Genistein	-7.5	-7.4	-6.1	-8.7	-8	-9.8	-10.7	-6.5
7	Piperine	-7.3	-8	-6.2	-8.6	-7.8	-8.8	-10.3	-6.1
8	Epicatechin-3-gallate	-7.9	-7.4	-6.1	-8.5	-8.8	-8.4	-8.8	-6.7
9	Curcumol	-6.2	-6.2	-5	-7.5	-7.1	-7	-6	-5.4
10	Berbamine	-6.9	-6.9	-5.7	-5.7	-6.6	-4.6	-6.7	-7.5
11	β-Boswellic acid	-7	-8	-5.6	-4.8	-6.7	-5.8	-7.6	-6.4
12	Paeoniflorin	-7.4	-7.5	-5.7	-9.1	-9.1	-6.6	-9.1	-6.6
13	Resveratrol	-7.5	-8	-5.8	-7.7	-8	-9.3	-9.4	-5.8
14	Ferulic acid	-6.7	-6.9	-4.7	-6.8	-6.8	-7.2	-7.6	-4.9
15	Thymoquinone	-6.8	-6.8	-4.3	-6.8	-6.6	-7.3	-6.8	-4.7
16	Quercetin	-6.9	-8.4	-5.8	-9.1	-8.8	-9.2	-9.9	-5.7
17	Rutin	-7.9	-8.1	-5.3	-9.4	-8.8	-7.8	-8.1	-6.4
18	Kaempferol	-6.7	-8.4	-5.9	-8.6	-8.8	-9.2	-9.4	-5.8
19	β-sitosterol	-8.3	-7.2	-5.8	-8.3	-9.1	-7.7	-7.4	-6.8
20	Sinomenin	-6.8	-6.1	-5.4	-7.1	-5.3	-6.9	-6.3	-5.2
21	Colchicine	-6.9	-6	-5.7	-4.5	-7.2	-6.3	-5.9	-5.8
22	Bartogenic acid	-6.8	-7.5	-5.5	-5.2	-6.3	-6.3	-8	-6.5
23	Cedrol	-6.3	-7.8	-5	-7	-6.9	-6.2	-6	-5.6
24	Nicotine	-6.7	-6.3	-4.3	-6	-6	-6.7	-6.8	-4.5
25	Celastrol	-7.5	-8.9	-5.6	-5.8	-6.5	-7.6	-7.9	-7.9
26	Chebulanin	-8.2	-7.8	-5.3	-8	-8.8	-6.1	-7.9	-5.9
27	Salvianolic acid B	-7.7	-7	-5.8	-10	-9.5	-5.7	-9.6	-6.8
28	Internal ligand	-8.9	-7.3	-4	-8.3	-6.6	-10.4	-10.4	-6.6
29	Methotrexate	-6.6	-7.8	-6.5	-9.0	-6.7	-9.0	-9.5	-6.3

Against JAK-2 receptor (pdb: 3e62), sanguinarine was found to be the most active phytoconstituent with the binding affinity -10.1 kcal/mol. In the docking results, the binding pose analysis showed that this compound formed hydrogen bonds with amino acids LEU855, GLY858, LEU932, ARG980 and hydrophobic interactions *viz*. π-σ, alkyl and π-alkyl bonding with VAL863, LEU983, LEU855, ALA880 residues (Figure 8).

Further, genistein was the most active compound against the MAPK-14 (pdb: 4f9y) receptor with the binding affinity of -9.8 kcal/mol, comparable to the internal ligand. Genistein showed the various interactions with the target, like hydrogen bonds with amino acids SER293, SER251, LEU195; carbon-hydrogen bond with SER252; hydrophobic **π-σ** interactions with LEU246, ILE250, four **π-π** stacked interactions with TRP197, **π-alkyl with amino acids** LEU195, ILE250, ALA255, LYS249 (Figure 9).

Hesperidin was screened out as the best phytoconstituent against the MMP9 (pdb:3esm) receptor protein. Because of hydroxyl groups in its structure, hesperidin interacted in the active site of the target by hydrogen bonding with amino acids MET247, HIS230, ALA189, GLN227; carbon-hydrogen bond with PRO246; **π-donor hydrogen bond** ARG249 and HIS230. This compound also showed **π-σ** hydrophobic interactions with HIS226, LEU188, LEU243, **π-π stacked hydrophobic interactions with HIS226, alkyl**, and π-alkyl hydrophobic interactions with LEU243 and ARG249 amino acids (Figure 10).

Further, hecogenin showed the highest binding score (-8.3 kcal/mol) against TNF-α (pdb: 2az5) among the 27 phytoconstituents. This compound made hydrophobic interactions with amino acids TYR59, HIS15, and TYR119 of the active site of the receptor (Figure 11).

3.3 ADME Prediction Study

ADME profile of the selected eight phytoconstituents was predicted with SwissADME[46] and compiled in Table 4. As per the results, all the phytoconstituents have low iLOGP value; hence, it was expected that these molecules would show good absorption. In addition, all the phytoconstituents were predicted to be soluble to moderately soluble with high Gastrointestinal (GI) absorption except hesperidin, naringenin and epicatechin-3-gallate. Further, most of the molecules are not inhibitors of CYP2C19, CYP2C9, CYP2D6, CYP3A4, members of the liver enzymes cytochrome

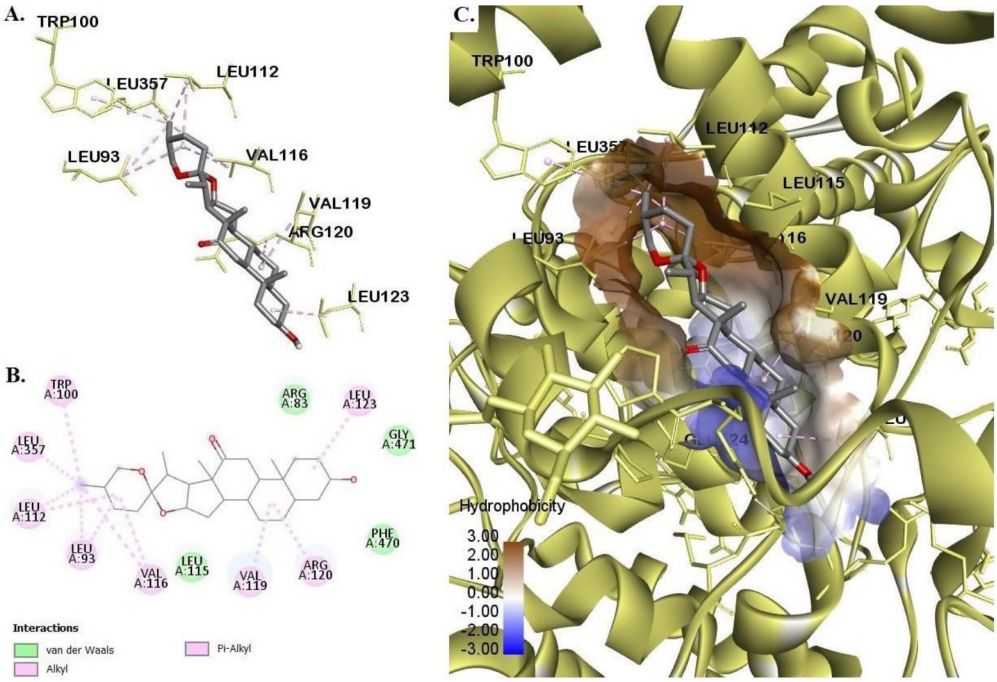


Figure 4. The binding pose of hecogenin with COX-1 (pdb:3n8z): Panel A shows 3D interactions, Panel B shows 2D interactions, and Panel C shows the compound docked in the active site of the protein.

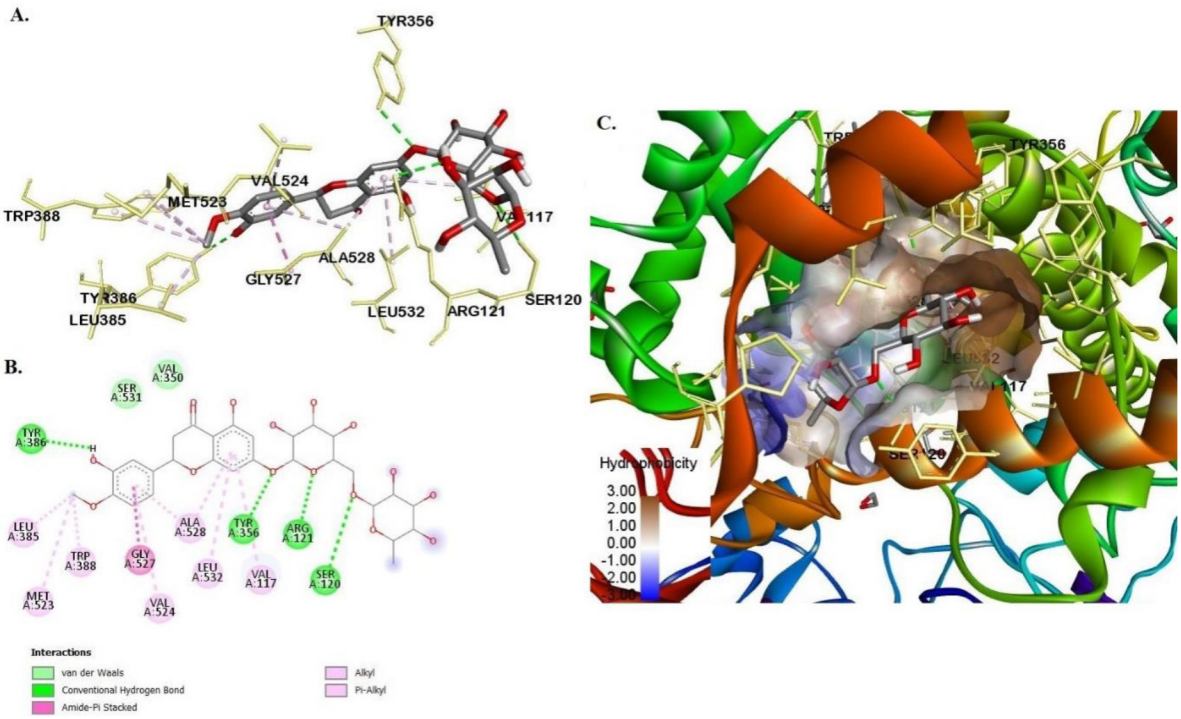


Figure 5. The binding pose of hesperidin with COX-2 (pdb: 4ph9): Panel A shows 3D interactions, Panel B shows 2D interactions, and Panel C shows the compound docked in the active site of the protein.

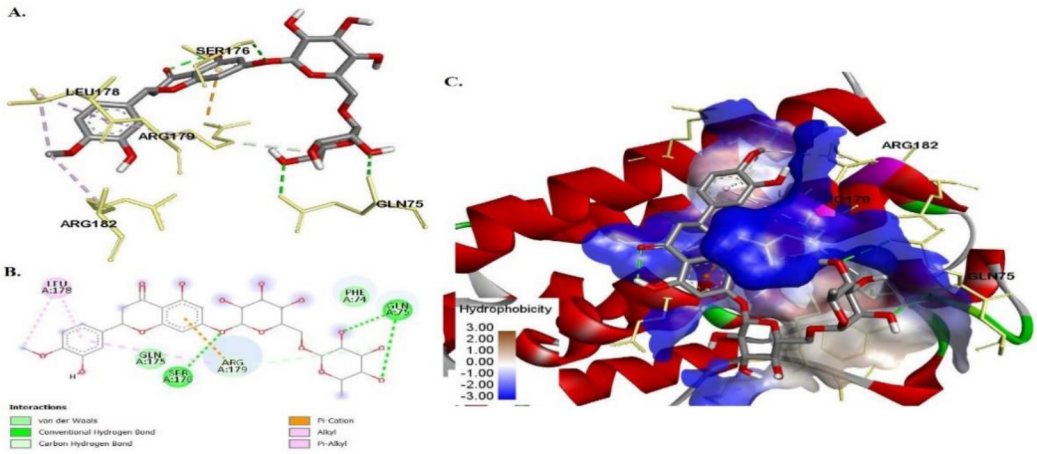


Figure 6. The binding pose of hesperidin with IL-6 (pdb: 1alu): Panel A shows 3D interactions, Panel B shows 2D interactions, and Panel C shows the compound docked in the active site of the protein.

P450, which have an important role in drug metabolism. So, it can be predicted that these molecules will not accumulate in the body, but at the same time, they can be metabolised at a fast rate[61]. Log Kp (cm/s) is the skin permeation ability of the molecule across the stratum corneum. The skin permeability of a molecule depends upon the log $K_{o/w}$ (octanol-water partition coefficient) and molecular weight. The higher the negative value of Log Kp, the less the drug is expected to permeable for stratum corneum layer of skin[62]. According to results, Sanguinarine, hecogenin, berberine, and piperine were predicted to be more skin permeable as compared to hesperidin and naringenin. Moreover, the molecules were also screened for Egan[50], Ghose[51], Lipinski[52], Muegge[53] and Veber[54] rules. Sanguinarine, hecogenin, berberine, genistein and piperine followed

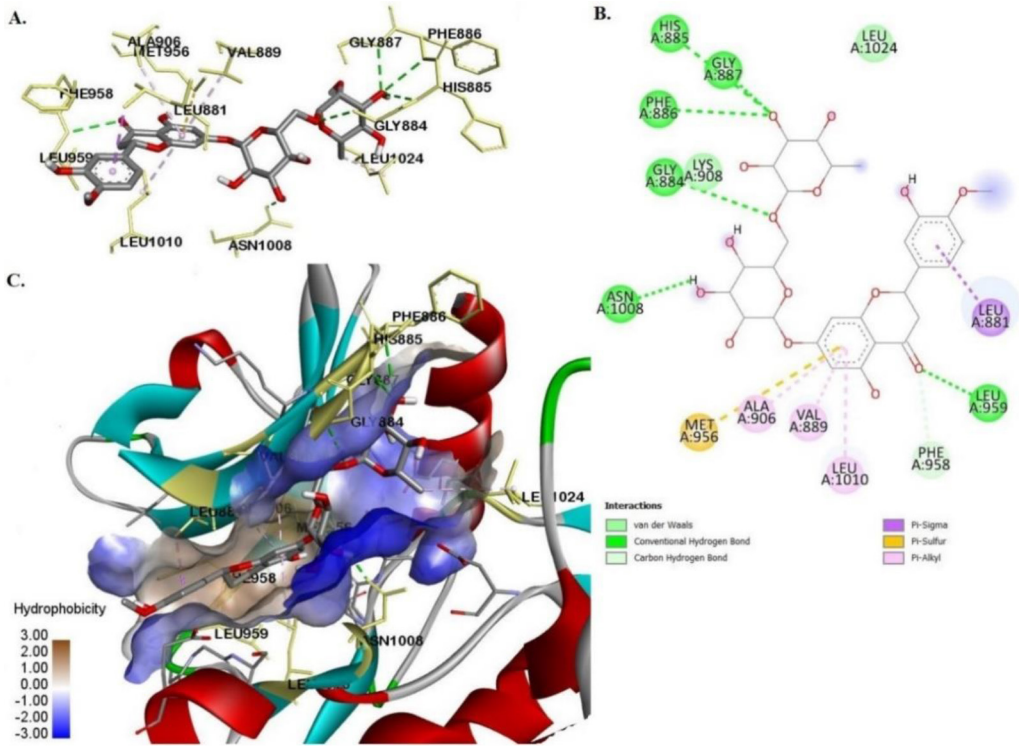


Figure 7. The binding pose of hesperidin with JAK-1 (pdb: 4ehz): Panel A shows 3D interactions, Panel B shows 2D interactions, and Panel C shows the compound docked in the active site of the protein.

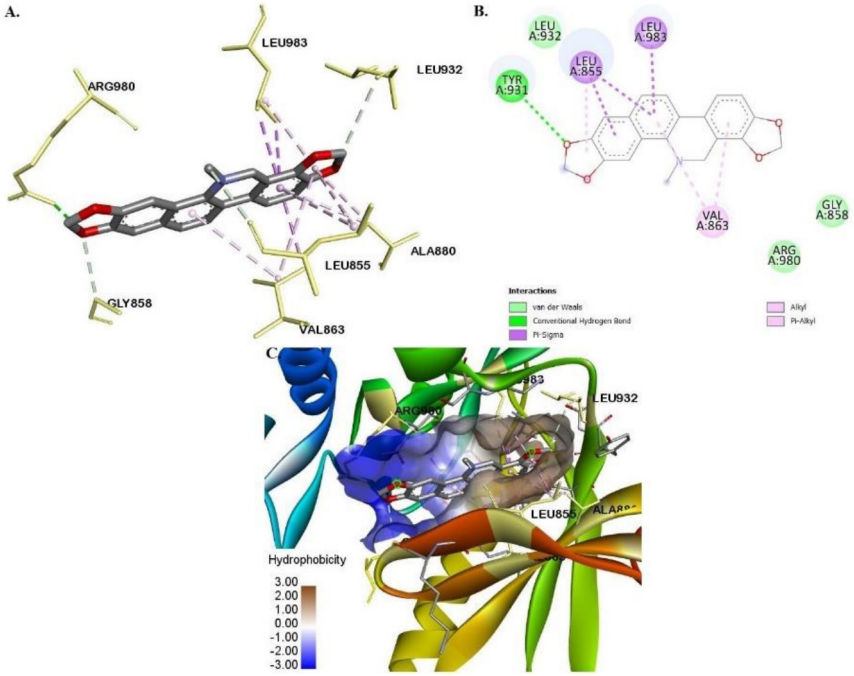


Figure 8. The binding pose of sanguinarine with JAK-2 (pdb: 3e62): Panel A shows 3D interactions, Panel B shows 2D interactions, and Panel C shows the compound docked in the active site of the protein.

all the criteria of the mentioned rules, while others have shown deviation in some of the criteria. Most of the molecules fulfilled the criteria of leadlikeness with one or two violations, which means these molecules have the ability to provide a lead molecule for further studies.

3.4 Bioactive Score

The complex balance of several molecular properties like hydrophobicity, hydrogen bonding characteristics, electronic distribution, flexibility and molecule size and pharmacophoric features that determines whether a given molecule is similar to the recognised drugs, is known as drug likeness or drugability. These properties also affect the bioavailability of the drug, transport properties, protein binding, reactivity, toxicity, metabolic stability and many others. Molinspiration web tool was used to predict bioactivity score that is

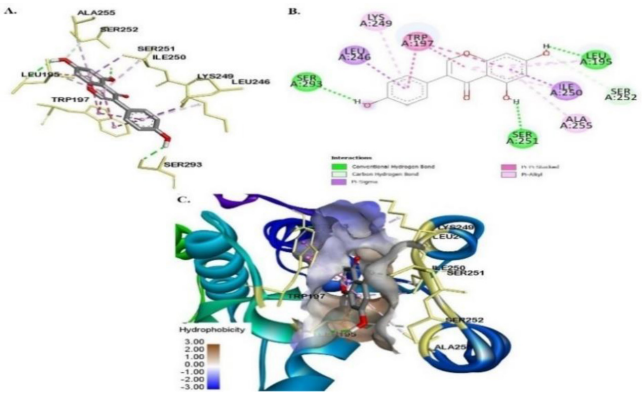


Figure 9. The binding pose of genistein with MAPK-14 (pdb: 4f9y): Panel A shows 3D interactions, Panel B shows 2D interactions, and Panel C shows the compound docked in the active site of the protein.

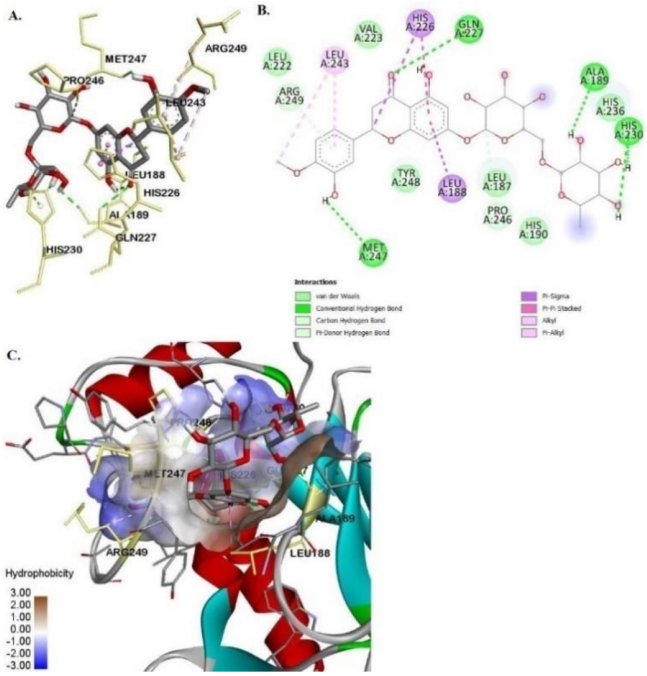


Figure 10. The binding pose of hesperidin with MMP9 (pdb: 3esm): Panel A shows 3D interactions, Panel B shows 2D interactions, and Panel C shows the compound docked in the active site of the protein.

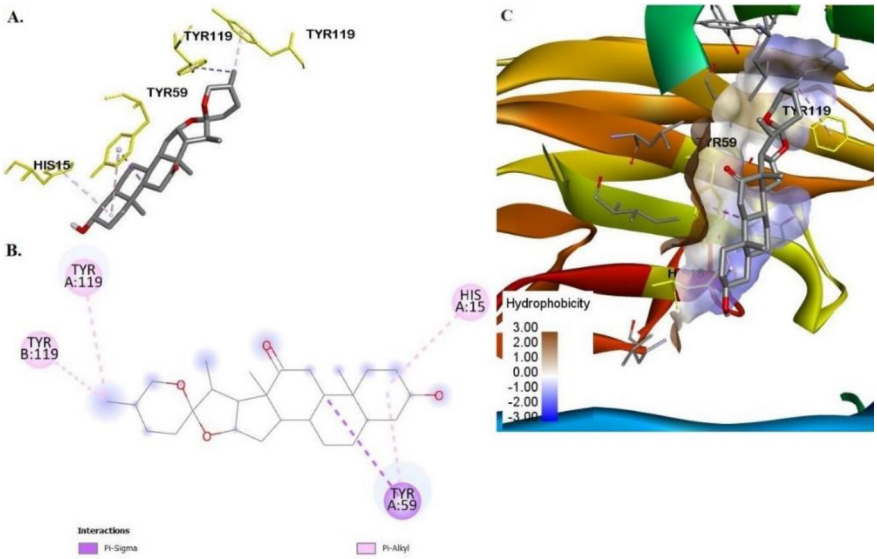


Figure 11. The binding pose of hecogenin with TNF-α (pdb: 2az5): Panel A shows 3D interactions, Panel B shows 2D interactions, and Panel C shows the compound docked in the active site of the protein.

Table 4. ADME results of the selected phytoconstituents from SwissADME

Molecule	Hesperidin	Sanguinarine	Hecogenin	Berberine	Naringenin	Genistein	Piperine	Epicatechin-3-gallate
MW	610.56	332.33	430.62	336.36	580.53	270.24	285.34	442.37
#Heavy atoms	43	25	31	25	41	20	21	32
#Aromatic heavy atoms	12	18	0	16	12	16	6	18
Fraction Csp3	0.54	0.15	0.96	0.25	0.52	0	0.35	0.14
#Rotatable bonds	7	0	0	2	6	1	4	4
#H-bond acceptors	15	4	4	4	14	5	3	10
#H-bond donors	8	0	1	0	8	3	0	7
MR	141.41	94.68	122.27	94.87	134.91	73.99	85.47	110.04
TPSA	234.29	40.8	55.76	40.8	225.06	90.9	38.77	177.14
iLOGP	2.6	-0.04	4.06	0	2.38	1.91	3.38	1.44
XLOGP3	-0.14	4.45	4.83	3.62	-0.44	2.67	3.46	1.53
WLOGP	-1.48	3.43	4.97	3.1	-1.49	2.58	2.51	2.2
MLOGP	-3.04	2.72	4.09	2.19	-2.77	0.52	2.39	0.05
Silicos-IT Log P	-1.55	3.85	3.99	3.74	-1.64	2.52	3.41	1.04
Consensus Log P	-0.72	2.88	4.39	2.53	-0.79	2.04	3.03	1.25
ESOL Class	Soluble	Moderately soluble	Moderately soluble	Moderately soluble	Soluble	Soluble	Soluble	Soluble
Ali Class	Moderately soluble	Moderately soluble	Moderately soluble	Moderately soluble	Soluble	Moderately soluble	Soluble	Moderately soluble
Silicos-IT class	Soluble	Poorly soluble	Moderately soluble	Moderately soluble	Soluble	Moderately soluble	Soluble	Soluble
GI absorption	Low	High	High	High	Low	High	High	Low
BBB permeant	No	Yes	Yes	Yes	No	No	Yes	No
Pgp substrate	Yes	Yes	Yes	Yes	Yes	No	No	No
CYP1A2 inhibitor	No	Yes	No	Yes	No	Yes	Yes	No
CYP2C19 inhibitor	No	Yes	No	No	No	No	Yes	No
CYP2C9 inhibitor	No	No	No	No	No	No	Yes	No
CYP2D6 inhibitor	No	No	No	Yes	No	Yes	No	No
CYP3A4 inhibitor	No	No	No	Yes	No	Yes	No	No
log Kp (cm/s)	-10.12	-5.17	-5.5	-5.78	-10.15	-6.05	-5.58	-7.91
Lipinski #	3	0	0	0	3	0	0	1
Ghose #	4	0	1	0	4	0	0	0
Veber #	1	0	0	0	1	0	0	1
Egan #	1	0	0	0	1	0	0	1
Muegge #	4	0	0	0	3	0	0	2
Bioavailability Score	0.17	0.55	0.55	0.55	0.17	0.55	0.55	0.55
PAINS #alerts	0	0	0	0	0	0	0	1
Brenk #alerts	0	2	0	1	0	0	2	1
Leadlikeness#	1	1	2	1	1	0	0	1
Synthetic Accessibility	6.34	2.59	6.7	3.14	6.16	2.87	2.92	4.16

#violations

Table 5. Bioactivity score of the selected phytoconstituents using Molinspiration

S. No.	Compound	GPCR ligand	Kinase inhibitor	Ion channel modulator	Protease inhibitor	Nuclear receptor ligand	Enzyme inhibitor
1	Hesperidin	-0.01	-0.36	-0.59	0	-0.2	0.06
2	Sanguinarine	-0.03	0.17	0.5	-0.14	-0.76	0.54
3	Hecogenin	0.05	-0.57	0.04	0.08	0.47	0.61
4	Berberine	-0.11	-0.27	0.71	-0.35	-0.78	0.82
5	Naringin	0.11	-0.24	-0.4	0.09	0.04	0.24
6	Genistein	-0.22	-0.06	-0.54	-0.68	0.23	0.13
7	Piperine	0.15	-0.13	-0.18	-0.1	-0.13	0.04
8	Epicatechin-3-gallate	0.17	0.05	0.02	0.13	0.34	0.25

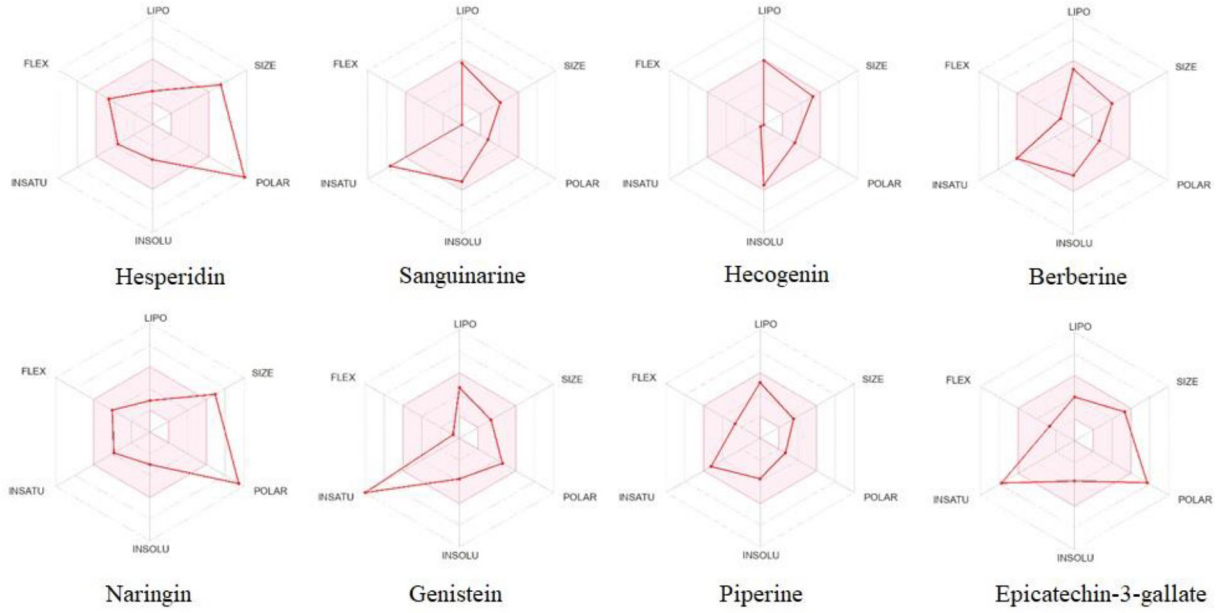


Figure 12. Bioavailability radar of selected molecules.

Table 6. Toxicity of the selected phytoconstituents

S. No.	Molecule	Predicted LD50	Predicted toxicity class	Hepato-toxicity (probability)	Carcinogenicity (probability)	Immuno-toxicity (probability)	Muta-genicity (probability)	Cyto-toxicity (probability)
1	Hesperidin	12000mg/kg	5	Inactive (0.81)	Inactive (0.93)	Active (0.99)	Inactive (0.9)	Inactive (0.52)
2	Sanguinarine	778mg/kg	4	Inactive (0.75)	Active (0.54)	Active (0.98)	Active (0.66)	Inactive (0.6)
3	Hecogenin	10000mg/kg	5	Active (0.5)	Inactive (0.72)	Active (0.97)	Inactive (0.87)	Inactive (0.77)
4	Berberine	200mg/kg	3	Inactive (0.82)	Active (0.56)	Active (0.99)	Active (0.62)	Active (0.96)
5	Naringin	2300mg/kg	5	Inactive (0.81)	Inactive (0.9)	Active (0.99)	Inactive (0.73)	Inactive (0.66)
6	Genistein	2500mg/kg	5	Inactive (0.69)	Inactive (0.69)	Inactive (0.97)	Inactive (0.74)	Inactive (0.91)
7	Piperine	330mg/kg	4	Inactive (0.91)	Active (0.53)	Active (0.96)	Inactive (0.96)	Inactive (0.53)
8	Epicatechin-3-gallate	1000mg/kg	4	Inactive (0.7)	Inactive (0.54)	Inactive (0.87)	Inactive (0.7)	Inactive (0.82)

used to analyse the drugability properties of molecule as GPCR ligand, KI, ICM, PI, NRL and EI. The molecules with a score greater than 0 the molecule was supposed to be highly active, scores between -0.5 to -0.0 denote moderate activity, and scores lower than -0.5 means inactivity. According to the results, epicatechin-3-gallate exhibited good activity against all the enzymes. Other molecules also displayed moderate activity, as seen in Table 5.

3.5 Bioavailability Radar

Bioavailability radar is a rapid assessment for the oral bioavailability of the compound. As seen in Figure 12, the pink area displayed the ideal range of lipophilicity, size, solubility, polarity, flexibility, and insaturation of the molecule. When all the criteria of the molecule fall in the pink area of the radar plot, the molecule is considered to be orally bioavailable. Lipophilicity and molecular size determined the absorption of the molecule. High molecular weight and high flexibility of the compound with low polar surface area reduced the oral bioavailability. As per the results, three phytoconstituents, hecogenin, berberine, and piperine, were noted to satisfy the radar plot criteria and were recommended to be orally bioavailable. Though other molecules do not satisfy some of the criteria. But there are more chances to modify these molecules to make them orally bioavailable.

3.6 Toxicity

The toxicity of the molecule is another important assessment in the drug design process. In this study, toxicity analysis, like LD50, hepatotoxicity, carcinogenicity, immunotoxicity, mutagenicity, and cytotoxicity, was predicted with Protox-II. Chemical were categorized from class 1-6 according to LD50; Class 1: fatal if swallowed (LD50≤ 5mg/kg); Class 2: fatal if swallowed (5mg/kg<LD50≤50mg/kg); Class 3: toxic if swallowed (50mg/kg<LD50 ≤300mg/kg); Class 4: harmful if swallowed (300mg/kg<LD50≤2000mg/kg); Class 5: may be harmful if swallowed (2000mg/kg< LD50≤5000mg/kg); Class 6: Non-toxic.

Protox-II evaluated the toxicity endpoints according to a predictive model based on Ames bacterial mutation, *in vitro* Tox21 tests, hepG2 cytotoxicity assay, and *in vivo* cytotoxicity, mutagenicity assay. As seen in Table 6, genistein and epicatechin-3-gallate showed inactive prediction for all with good probability. Hesperidin and piperine were predicted to have immunotoxicity, whereas sanguinarine and berberine were found to be active for carcinogenicity, immunotoxicity, mutagenicity and cytotoxicity. Both Hecogenin and naringenin were predicted as active for immunotoxicity. There is significant debate on the immunotoxicological response of phytoconstituents that modulate immunity. Although there are many therapeutic advantages to immune functioning modification, there is also a risk of immunotoxicity, including cytokine storms, hypersensitivity, and allergic reactions[63]. The successful development of a drug with immunomodulatory potential may be facilitated by an understanding of the immunomodulatory mechanism through the use of docking simulation.

4. Conclusion

Based on our analysis, eight phytoconstituents, hesperidin, sanguinarine, hecogenin, berberine, naringin, genistein, piperine, and epicatechin-3-gallate, possessed good binding affinity with all the studied receptors. Their binding affinity was found to be even better than the standard drug, methotrexate. The pharmacokinetics and toxicity studies showed good GI absorption with less toxicity. Though some molecules displayed immunomodulation but it can be beneficial in autoimmune diseases like rheumatoid arthritis. The phytoconstituents were also found to have drug-like and lead-like properties. These molecules also showed moderate activity as G-Protein Coupled Receptors (GPCR) ligand, kinase inhibitor, ion channel modulator, protease inhibitor, nuclear receptor ligand, and enzyme inhibitor. This reveals that bioactive compounds have the ability to bind with these receptors, causing modulation of immune factors, which in turn hinders rheumatoid arthritis. Further investigation is still going on in our lab to establish the formulation with the possible combination of these phytoconstituents for effective treatment of rheumatoid arthritis.

5. Author Contribution

Conceptualisation and visualisation- Preeti Maan; Methodology, and software - Shilpi Chauhan and Preeti Maan; Original draft preparation - Shilpi

Chauhan and Preeti Maan; Supervision- Dimpy Rani; Review and editing - Nisha Gupta. All authors have read and agreed to the published version of the manuscript.

6. References

1. Gravallese EM, Firestein GS, Koscal N, Ling E, Longo DL, Messenger LA, *et al*. What is rheumatoid arthritis? N Engl J Med. 2024; 390(13):e32. https://doi.org/10.1056/NEJMp2310178 PMid:38598569
2. Guo L, Wang J, Li J, Yao J, Zhao H. Biomarkers of rheumatoid arthritis-associated interstitial lung disease: A systematic review and meta-analysis. Front Immunol. 2024; 15:1455346. https://doi.org/10.3389/fimmu.2024.1455346 PMid:39534599 PMCid:PMC11554464
3. Atzeni F, Talotta R, Masala IF, Gerardi MC, Casale R, Sarzi-Puttini P. Central nervous system involvement in rheumatoid arthritis patients and the potential implications of using biological agents. Best Pract Res Clin Rheumatol. 2018; 32(4):500-510. https://doi.org/10.1016/j.berh.2019.02.003.
4. Cieza A, Causey K, Kamenov K, Hanson SW, Chatterji S, Vos T. Global estimates of the need for rehabilitation based on the Global Burden of Disease study 2019: A systematic analysis for the Global Burden of Disease Study 2019. Lancet. 2021; 396(10267):2006-2017. https://doi.org/10.1016/S0140-6736(20)32340-0 PMid:33275908
5. Deane KD, Demoruelle MK, Kelmenson LB, Kuhn KA, Norris JM, Holers VM. Genetic and environmental risk factors for rheumatoid arthritis. Best Pract Res Clin Rheumatol. 2017; 31(1):3-18. https://doi.org/10.1016/j.berh.2017.08.003.
6. Jang S, Kwon EJ, Lee JJ, Spinelli R, Pecani A, Jang S, *et al*. Rheumatoid arthritis: Pathogenic roles of diverse immune cells. Int J Mol Sci. 2022; 23(2):905. https://doi.org/10.3390/ijms23020905 PMid:35055087 PMCid:PMC8780115
7. Yoshitomi H. Regulation of immune responses and chronic inflammation by fibroblast-like synoviocytes. Front Immunol. 2019; 10:1395. https://doi.org/10.3389/fimmu.2019.01395 PMid:31275325 PMCid:PMC6593115
8. Gravallese EM, Firestein GS. Rheumatoid arthritis - common origins, divergent mechanisms. N Engl J Med2023; 388(6):529-542. https://doi.org/10.1056/NEJMra2103726 PMid:36780677
9. Kim J, Jung KH, Yoo J, Park JH, Yan HH, Fang Z, *et al*. PBT-6, a novel PI3KC2γ inhibitor in rheumatoid arthritis. Biomol Ther (Seoul). 2020; 28(2):172-183. https://doi.org/10.4062/biomolther.2019.153 PMid:31739383 PMCid:PMC7059814
10. Nakayamada S, Kubo S, Iwata S, Tanaka Y. Chemical JAK inhibitors for the treatment of rheumatoid arthritis. Expert Opin Pharmacother. 2016; 17(16):2215-2225. https://doi.org/10.1080/14656566.2016.1241237 PMid:27690665
11. Molteni E, Adinolfi A, Bondi V, Delvino P, Sakellariou G, Trentanni C, *et al*. Novel insights into the management of rheumatoid arthritis: One year in review 2024. Clin Exp Rheumatol. 2024; 42(5):947-960. https://doi.org/10.55563/clinexprheumatol/166dsf PMid:38743447
12. Crofford LJ. Use of NSAIDs in treating patients with arthritis. Arthritis Res Ther. 2013; 15(Suppl 3):S2. https://doi.org/10.1186/ar4174 PMid:24267197 PMCid:PMC3891482
13. Thabitha A, Ali AMMT, Kumari SS, Rakhi, Swami V, Priya AM, *et al*. Targeting IL-17 and IL-17D receptors of rheumatoid arthritis using phytocompounds: A molecular docking study. IOP Conf Ser Mater Sci Eng. 2017; 263(2):022040. https://doi.org/10.1088/1757-899X/263/2/022040
14. Saini D, Madan K, Chauhan S. Screening of phytoconstituents from traditional plants against sarscov- 2 using molecular docking approach. Lett Drug Des Discov. 2022; 19(11):1022-1038. https://doi.org/10.2174/1570180819666220307163058
15. ProtParam. Swiss Institute of Bioinformatics. https://web.expasy.org/protparam/
16. Gasteiger E, Hoogland C, Gattiker A, Duvaud S, Wilkins MR, Appel RD, *et al*. Protein identification and analysis tools on the ExPASy Server. The Proteomics Protocols Handbook; 2005. p. 571-607. https://doi.org/10.1385/1-59259-890-0:571
17. Debnath A, Sengupta A, Rudrapal S, Kumar A, Rani M. *In-silico* study of molecular adaptations in halophilic Cas9. Lett Appl Microbiol. 2025; 78(2):ovaf006. https://doi.org/10.1093/lambio/ovaf006 PMid:39832801
18. Chintakunta R, Meka G. Synthesis, *in silico* studies and antibacterial activity of some novel 2-substituted benzimidazole derivatives. Futur J Pharm Sci. 2020; 6:128. https://doi.org/10.1186/s43094-020-00144-9
19. Sidhu RS, Lee JY, Yuan C, Smith WL. Comparison of cyclooxygenase-1 crystal structures: cross-talk between monomers comprising cyclooxygenase-1 homodimers. Biochemistry. 2010; 49(33):7069-7079. https://doi.org/10.1021/bi1003298 PMid:20669977 PMCid:PMC2932651
20. Orlando BJ, Lucido MJ, Malkowski MG. The structure of ibuprofen bound to cyclooxygenase-2. J Struct Biol. 2015; 189(1):62-66. https://doi.org/10.1016/j.jsb.2014.11.005.
21. Somers W, Stahl M, Seehra JS. 1.9 A crystal structure of interleukin 6: Implications for a novel mode of receptor dimerization and signaling. EMBO J. 1997; 16(5):989-997. https://doi.org/10.1093/emboj/16.5.989 PMid:9118960 PMCid:PMC1169699
22. Zak M, Mendonca R, Balazs M, Barrett K, Bergeron P, Blair WS, *et al*. Discovery and optimization of C-2 methyl imidazopyrrolopyridines as potent and orally bioavailable JAK1 inhibitors with selectivity over JAK2. J Med Chem. 2012; 55(13):6176-6193. https://doi.org/10.1021/jm300628c
23. Antonysamy S, Hirst G, Park F, Sprengeler P, Stappenbeck F, Steensma R, *et al*. Fragment-based discovery of JAK-2 inhibitors. Bioorg Med Chem Lett. 2009; 19(1):279-282. https://doi.org/10.1016/j.bmcl.2008.08.064 PMid:19019674

24. Watterson DM, Grum-Tokars VL, Roy SM, Schavocky JP, de Bradaric B, Bachstetter AD, *et al*. Development of novel *in vivo* chemical probes to address CNS protein kinase involvement in synaptic dysfunction. PLoS One. 2013; 8(6):e66226. https://doi.org/10.1371/journal.pone.0066226 PMid:23840427 PMCid:PMC3694096
25. Nuti E, Cuffaro D, Bernardini E, Camodeca C, Panelli L, Chaves S, *et al*. Development of thioaryl-based matrix metalloproteinase-12 inhibitors with alternative zinc-binding groups: synthesis, potentiometric, NMR, and crystallographic studies. J Med Chem. 2018; 61(10):4421-4435. https://doi.org/10.1021/acs.jmedchem.8b00096
26. He MM, Smith AS, Oslob JD, Flanagan WM, Braisted AC, Whitty A, *et al*. Small-molecule inhibition of TNF-alpha. Science. 2005; 310(5750):1022-1025. https://doi.org/10.1126/science.1116304 PMid:16284179
27. RCSB Protein Data Bank. RCSB.org. https://www.rcsb.org
28. Pettersen EF, Goddard TD, Huang CC, Couch GS, Greenblatt DM, Meng EC, *et al*. UCSF Chimera– A visualization system for exploratory research and analysis. J Comput Chem. 2004; 25(13):1605-1612. https://doi.org/10.1002/jcc.20084 PMid:15264254
29. Morris GM, Ruth H, Lindstrom W, Sanner MF, Belew RK, Goodsell DS, *et al*. AutoDock4 and AutoDockTools4: Automated docking with selective receptor flexibility. J Comput Chem. 2009; 30(16):2785-2791. https://doi.org/10.1002/jcc.21256 PMid:19399780 PMCid:PMC2760638
30. PubChem. National Center for Biotechnology Information. https://pubchem.ncbi.nlm.nih.gov/
31. O'Boyle NM, Banck M, James CA, Morley C, Vandermeersch T, Hutchison GR. Open Babel: An open chemical toolbox. J Cheminform. 2011; 3:33. https://doi.org/10.1186/1758-2946-3-33 PMid:21982300 PMCid:PMC3198950
32. Dallakyan S, Olson AJ. Small-molecule library screening by docking with PyRx. Methods Mol Biol. 2015; 1263:243-250. https://doi.org/10.1007/978-1-4939-2269-7_19 PMid:25618350
33. Zhang X, Chao P, Zhang L, Lu J, Yang A, Jiang H, *et al*. Integrating network pharmacology, molecular docking and simulation approaches with machine learning reveals the multi-target pharmacological mechanism of Berberis integerrima against diabetic nephropathy. J Biomol Struct Dyn. 2025; 43(4):2092-2108. https://doi.org/10.1080/07391102.2023.2294165 PMid:38379386
34. Zhang L, Zhu W. Screening antioxidant components in Yiwei decoction using spectrum-effect relationship and network pharmacology. J Anal Methods Chem. 2024; 2024(1):5514265. https://doi.org/10.1155/2024/5514265 PMid:39445127 PMCid:PMC11498994
35. Gangwar A, Tewari G, Pande C, Prakash O, Kanyal B, Tewari LM, *et al*. Effect of drying conditions on the chemical compositions, molecular docking interactions and antioxidant activity of *Hedychium spicatum* Buch.-Ham. Rhizome essential oil. Sci Rep. 2024; 14(1):28568. https://doi.org/10.1038/s41598-024-79712-5 PMid:39562660 PMCid:PMC11576735
36. Dassault Systèmes. Free Download: BIOVIA Discovery Studio Visualizer. https://discover.3ds.com/discovery-studio-visualizer-download
37. Cheng M, Li M, Zhang Y, Gu X, Gao W, Zhang S, *et al*. Exploring the mechanism of PPCPs on human metabolic diseases based on network toxicology and molecular docking. Environ Int. 2025; 196:109324. https://doi.org/10.1016/j.envint.2025.109324 PMid:39952201
38. Afridi MB, Sardar H, Serdaroğlu G, Shah SWA, Alsharif KF, Khan H. SwissADME studies and Density Functional Theory (DFT) approaches of methyl substituted curcumin derivatives. Comput Biol Chem. 2024; 112:108153. https://doi.org/10.1016/j.compbiolchem.2024.108153 PMid:39067349
39. Loganathan V, Ahamed A, Akbar I, Gerbu DG, Alodaini HA, Manilal A. Cu(II)-catalyzed synthesis of pyrazolo[3,4-b] pyridine derivatives and their potential antibacterial and cytotoxic activities with molecular docking, DFT calculation, and SwissADME analysis. ACS Omega. 2024; 10(1):1643-1656. https://doi.org/10.1021/acsomega.4c09524 PMid:39829459 PMCid:PMC11740132
40. Ertl P, Rohde B, Selzer P. Fast calculation of molecular polar surface area as a sum of fragment-based contributions and its application to the prediction of drug transport properties. J Med Chem. 2000; 43(20):3714-3717. https://doi.org/10.1021/jm000942e PMid:11020286
41. Daina A, Michielin O, Zoete V. ILOGP: A simple, robust, and efficient description of n-octanol/water partition coefficient for drug design using the GB/SA approach. J Chem Inf Model. 2014; 54(12):3284-3301. https://doi.org/10.1021/ci500467k PMid:25382374
42. XLOGP3 v 3.2.0 User Manual. Copyright year 2007, https://archive.org/details/manualzilla-id-6906183
43. Wildman SA, Crippen GM. Prediction of physicochemical parameters by atomic contributions. J Chem Inf Comput Sci. 1999; 39(5):868-873. https://doi.org/10.1021/ci990307l
44. Moriguchi I, Hirono S, Liu Q, Nakagome I, Matsushita Y. Simple method of calculating octanol/water partition coefficient. Chem Pharm Bull (Tokyo). 1992; 40(1):127-130. https://doi.org/10.1248/cpb.40.127
45. Moriguchi I, Hirano H, Nakagome I. Comparison of reliability of log P values for drugs calculated by several methods. Chem Pharm Bull (Tokyo). 1994; 42(4):976-978. https://doi.org/10.1248/cpb.42.976
46. Daina A, Michielin O, Zoete V. SwissADME: A free web tool to evaluate pharmacokinetics, drug-likeness and medicinal chemistry friendliness of small molecules. Sci Rep. 2017;

7:42717. https://doi.org/10.1038/srep42717 PMid:28256516 PMCid:PMC5335600
47. Delaney JS. ESOL: Estimating aqueous solubility directly from molecular structure. J Chem Inf Comput Sci. 2004; 44(3):1000-1005. https://doi.org/10.1021/ci034243x PMid:15154768
48. Ali J, Camilleri P, Brown MB, Hutt AJ, Kirton SB. Revisiting the general solubility equation: in silico prediction of aqueous solubility incorporating the effect of topographical polar surface area. J Chem Inf Model. 2012; 52(2):420-428. https://doi.org/10.1021/ci200387c PMid:22196228
49. Daina A, Zoete V. A BOILED-Egg to predict gastrointestinal absorption and brain penetration of small molecules. ChemMedChem. 2016; 11(11):1117-1121. https://doi.org/10.1002/cmdc.201600182 PMid:27218427 PMCid:PMC5089604
50. Egan WJ, Merz KM, Baldwin JJ. Prediction of drug absorption using multivariate statistics. J Med Chem. 2000; 43(21):3867-3877. https://doi.org/10.1021/jm000292e PMid:11052792
51. Ghose AK, Viswanadhan VN, Wendoloski JJ. A knowledge-based approach in designing combinatorial or medicinal chemistry libraries for drug discovery. 1. A qualitative and quantitative characterization of known drug databases. J Comb Chem. 1999; 1(1):55-68. https://doi.org/10.1021/cc9800071 PMid:10746014
52. Lipinski CA, Lombardo F, Dominy BW, Feeney PJ. Experimental and computational approaches to estimate solubility and permeability in drug discovery and development settings. Adv Drug Deliv Rev. 2001; 46(1-3):3-26. https://doi.org/10.1016/S0169-409X(00)00129-0 PMid:11259830
53. Muegge I, Heald SL, Brittelli D. Simple selection criteria for drug-like chemical matter. J Med Chem. 2001; 44(12):1841-1846. https://doi.org/10.1021/jm015507e PMid:11384230
54. Veber DF, Johnson SR, Cheng HY, Smith BR, Ward KW, Kopple KD. Molecular properties that influence the oral bioavailability of drug candidates. J Med Chem. 2002; 45(12):2615-2623. https://doi.org/10.1021/jm020017n PMid:12036371
55. Mukhopadhyay S, Roy C, Ghosh P. Spice components as modulating agents of P-glycoprotein - An *in-silico* study. Indian J Pharmacol. 2024; 56(3):214-219. https://doi.org/10.4103/ijp.ijp_299_23 PMid:39078186 PMCid:PMC11286101
56. 56.Molinspiration Cheminformatics. Molinspiration.com. Available from: https://www.molinspiration.com/
57. Ayar A, Aksahin M, Mesci S, Yazgan B, Gül M, Yıldırım T. Antioxidant, cytotoxic activity and pharmacokinetic studies by Swiss ADME, Molinspiration, Osiris and DFT of PhTAD-substituted dihydropyrrole derivatives. Curr Comput Aided Drug Des. 2021; 18(1):52-63. https://doi.org/10.2174/1573409917666210223105722 PMid:33622227
58. Alqaaf M, Nasution AK, Karim MB, Rumman MI, Sedayu MH, Supriyanti R, *et al*. Discovering natural products as potential inhibitors of SARS-CoV-2 spike proteins. Sci Rep. 2025; 15(1):200. https://doi.org/10.1038/s41598-024-83637-4 PMid:39747174 PMCid:PMC11697186
59. Arreola R, Quintero-Fabián S, Lopez-Roa RI, Flores-Gutierrez EO, Reyes-Grajeda JP, Carrera-Quintanar L, *et al*. Immunomodulation and anti-inflammatory effects of garlic compounds. J Immunol Res. 2015; 2015:401630. https://doi.org/10.1155/2015/401630 PMid:25961060 PMCid:PMC4417560
60. El Shanawany EE, Fouad EA, Keshta HG, Hassan SE, Hegazi AG, Abdel-Rahman EH. Immunomodulatory effects of *Moringa oleifera* leaves aqueous extract in sheep naturally co-infected with *Fasciola gigantica* and *Clostridium novyi*. J Parasit Dis. 2019; 43(4):583-591. https://doi.org/10.1007/s12639-019-01130-6 PMid:31749528 PMCid:PMC6841766
61. Zhao M, Ma J, Li M, Zhang Y, Jiang B, Zhao X, *et al*. Cytochrome p450 enzymes and drug metabolism in humans. Int J Mol Sci. 2021; 22(23):12808. https://doi.org/10.3390/ijms222312808 PMid:34884615 PMCid:PMC8657965
62. Chen CP, Chen CC, Huang CW, Chang YC. Evaluating molecular properties involved in transport of small molecules in *Stratum corneum*: A quantitative structure-activity relationship for skin permeability. Molecules. 2018; 23(4):911. https://doi.org/10.3390/molecules23040911 PMid:29662033 PMCid:PMC6017021
63. Zerdan MB, Moussa S, Atoui A, Assi HI. Mechanisms of immunotoxicity: Stressors and evaluators. Int J Mol Sci. 2021; 22(15):8242. https://doi.org/10.3390/ijms22158242 PMid:34361007 PMCid:PMC8348050